A Self-Controlled Mind is Reflected by Stable Mental Processing

Tobias Kleinert [1,2,3], Kyle Nash [2], Josh Leota [2], Thomas Koenig [4], Markus Heinrichs [1,5], Bastian Schiller [1,5]*

[1] Laboratory for Biological Psychology, Clinical Psychology and Psychotherapy, Albert-Ludwigs-University of Freiburg, Stefan-Meier-Straße 8, 79104 Freiburg, Germany.

[2] Department of Psychology, University of Alberta, T6G 2E9 Edmonton, AB, Canada.

[3] Department of Ergonomics, Leibniz Research Centre for Working Environment and Human Factors, 44139 Dortmund, Germany.

[4] Translational Research Center, University Hospital of Psychiatry, University of Bern, CH-3000, Bern, Switzerland.

[5] Freiburg Brain Imaging Center, University Medical Center, University of Freiburg, 79104 Freiburg, Germany.

* Corresponding author:

Bastian Schiller

schiller@psychologie.uni-freiburg.de

Albert-Ludwigs-University of Freiburg

Stefan-Meier-Straße 8, DE-79104 Freiburg

Abstract

Self-control–the ability to inhibit inappropriate impulses–predicts economic, physical, and psychological well-being. However, recent findings demonstrate low correlations among self-control measures, raising the questions what self-control actually is. Here, we examine the idea that people high in self-control show more stable mental processing, characterized by fewer, but longer lasting processing steps due to fewer interruptions by distracting impulses. To test this hypothesis, we relied on resting EEG microstate analysis, a method that provides access to the stream of mental processing by assessing the sequential activation of neural networks. Across two samples (N_1=58 male adults from Germany; N_2=101 adults from Canada [58 females]), the temporal stability of resting networks (i.e., longer durations and fewer occurrences) was positively associated with self-reported self-control and a neural index of inhibitory control, and negatively associated with risk-taking behavior. These findings suggest that stable mental processing represents a core feature of a self-controlled mind.

Keywords: self-control, EEG, microstates, neural networks, resting-state, response inhibition, risk-taking

Statement of Relevance

Self-control enables us to regulate our behavior in order to achieve long-term goals. Indeed, scientists have found that people with high self-control live happier and healthier lives. Yet, the differences between a self-controlled and an impulsive mind have remained unclear. Here, we analyze the relationship between self-report, neural, and behavioral measures of self-control and brain activity when a person's mind is free to wander and no task is at hand. We demonstrate that self-controlled individuals show fewer, but longer lasting mental processing steps. These results suggest that people with high self-control have more stable mental processes with fewer interrupting thoughts and impulses. Our findings illustrate that analyzing the mental flow of the "resting" brain can reveal crucial information on the nature of our minds. In the future, assessing individual differences in the stability of mental processing could be helpful in understanding and treating disorders associated with deficient self-control.

Self-control is a fundamental trait that relates to the regulation of behavior and has been

originally defined as the ability to inhibit impulses in order to achieve long-term goals

(Inzlicht et al., 2021). Research has confirmed the adaptive nature of self-control,

demonstrating that self-controlled individuals show increased economic, physical, and

psychological well-being (De Ridder et al., 2012; Tangney et al., 2004). However, recent

findings cast doubt on the validity of both the leading theoretical model of self-control

(i.e., the strength model; Vohs et al., 2021) and distinct self-control measures (e.g.,

Wennerhold et al., 2020). Furthermore, by conceptually focusing on the role of inhibitory

processes, research might have neglected other aspects of self-control (e.g., proactively

avoiding temptations, or using cognitive reconstruals to alter the experience of

temptations; see also Discussion, second paragraph, and Fujita, 2011; Inzlicht et al.,

2021). These issues raise questions about how well we have actually understood the

construct of self-control. Based on overlooked theoretical models and empirical findings,

which suggest that self-controlled individuals are less prone to distracting impulses, we

hypothesize that self-control is associated with a less distracted mind, characterized by

more stable and longer lasting mental processing steps. To test this hypothesis, we rely on

microstate analysis of resting-state electroencephalography (EEG; Bréchet et al., 2020; da

Cruz et al., 2020; Nagabhushan Kalburgi et al., 2020). This analysis provides access to

the stream of mental processing by assessing the sequential activation of (usually) four

large-scale brain networks at a millisecond resolution (for a review, see Michel &

Koenig, 2018). We speculate that the temporal stability (i.e., longer durations and fewer

occurrences) across the four network types indicates an individual's general mental

processing stability. In order to investigate mental processing free of context, we focus on analyzing task-independent brain networks.

The strength model holds that self-control is a domain-general resource with a limited capacity that varies in individual strength, and that high self-control demands lead to depletion of this resource, as indicated by performance decreases during consecutive tasks (Baumeister et al., 2007). However, recent meta-analyses have shown that this depletion effect is much smaller than previously thought (e.g., Vohs et al., 2021), leaving a gap within self-control theory. If self-control is not a limited resource, what is it then? To answer this question, it could help to look at how researchers have measured this construct. Self-report measures like the Brief Self-Control Scale (BSCS) capture cognitively available aspects of self-control by having participants respond to items like "I am good at resisting temptation" (Tangney et al., 2004). Incentivized risk tasks, like the Balloon Analogue Risk Task (BART; Lejuez et al., 2002), indirectly assess self-control by having participants choose between smaller, but secure, and larger, but insecure monetary gains. Finally, researchers have analyzed inhibitory control related brain activity during both task-independent and task-dependent processing, arguing that neural measures may provide the most direct indices of self-control. An example is the baseline activation in inhibitory control-related brain regions (Schiller et al., 2014) and the NoGo-P300 amplitude, a task-dependent, neural index of inhibitory control, registered while participants are inhibiting pre-potent motor responses (Nash et al., 2013). In sum, while existing self-report, behavioral and neural measures of self-control choose different routes to access the construct, they share the assumption that self-control relates to inhibitory capacity. Yet, associations among these measures are commonly weak to

absent (Wennerhold et al., 2020). The ongoing confusion about the "right" way to measure self-control emphasizes the need to reconceptualize the construct by identifying other core features of self-control across measures.

Here, we argue that a core feature of self-control is stable mental processing characterized by fewer, but longer lasting mental processing steps due to fewer interruptions by distracting impulses. This hypothesis is based on three main pieces of suggestive theoretical and empirical evidence. *First*, different measures of self-control share the notion that a self-controlled mind is able to shield against mental "interruptions" like distracting events or impulsive urges in order to maintain a stable, higher-order goal (Schiffer et al., 2015). For example, scoring high on the item "Sometimes I can't stop myself from doing something, even if I know it is wrong" will result in a lower score in the BSCS (Tangney et al., 2004). In line with this notion, the Continuous Performance Test (CPT) measures the ability to quickly respond to specific stimuli while neglecting distracting ones (Fallgatter et al., 1997). Moreover, in incentivized risk tasks participants have to resist the impulse to obtain potential immediate high-gain rewards in order to maximize their long-term profit (Lejuez et al., 2002). *Second*, research on Attention Deficit Hyperactivity Disorder (ADHD), a mental disorder associated with deficient self-control, suggests that an "uncontrolled mind" is reflected by unstable mental processing prone to interruption by distracting impulses (Castellanos et al., 2006). Specifically, the inability to distinguish between relevant and irrelevant information is assumed to lead to increased vulnerability for insignificant information to intrude into the current mental process (Fassbender et al., 2009). These deficiencies impair performance in objective self-control measures, as evident by more

errors and more variable response times in the CPT (Epstein et al., 2003), and more

impulsive decision-making in the BART (Humphreys & Lee, 2011). *Third*, it has been

observed that self-control is negatively associated with mind-wandering ($r=-.49$, $p<.001$),

a mental processing style characterized by many interruptions of mental processing and

consequently shorter processing steps (Deng et al., 2019). In sum, a broad array of

research supports the theoretical assumption that a core feature of self-control is stable

mental processing. But how can we actually gain access to an individual's mental

processing style to test this hypothesis?

An ideal tool to identify mental processing steps on a millisecond scale is EEG

microstate analysis (Michel & Koenig, 2018). Microstate analysis uses clustering of

electrophysiological data to obtain a sequential activation of large-scale brain networks

and quantify their temporal characteristics (e.g., average duration, average occurrences

per second). This approach is consistent with the notion that self-control is associated

with the activation of whole brain neural networks (Schiller & Delgado, 2010).

Microstates arise due to simultaneous activation of specific neuronal assemblies and thus

reflect temporarily stable episodes of coherent mental activity (Michel & Koenig, 2018).

Based on the idea that microstates represent the individual units that constitute the stream

of mental processing, each microstate may be described as a distinct mental processing

step. In the resting brain, microstates remain stable for approximately 40-120ms before

quickly changing into other networks (Lehmann et al., 1987). Further illustrating their

fundamental character, four prototypical types of microstate networks (A-D) account for

approximately 80% of the variance in resting EEG recordings of almost every single

individual (Michel & Koenig, 2018). Importantly, the average duration of microstate

networks in milliseconds and their average number of occurrences per second are highly

correlated across microstate types (duration: $r=.79$; occurrence: $r=.51$; Khanna et al.,

2014). This suggests that individuals have a general tendency for more (fewer, but longer

lasting microstates) or less (more, but shorter lasting microstates) stable mental

processing at rest (beyond associations of specific microstates' stability with different

levels of consciousness, neuropsychiatric conditions, and cognitive contents; for a

review, see Michel & Koenig, 2018).

Here, we investigated the hypothesis that self-report, neural and behavioral

measures of self-control show associations with stable mental processing, although these

measures may not correlate with each other (Wennerhold et al., 2020). In Study 1, we

first tested for associations of stable mental processing with self-reported self-control

(BSCS; Tangney et al., 2004) in 58 healthy men. Second, we tested for associations with

a neural index of inhibitory control (the NoGo-P300 in the CPT (Fallgatter et al., 1997).

Third, we localized neural sources of inhibitory control and investigate if stable mental

processing is associated with cortical activity in these sources (using sLORETA; Pascual-

Marqui, 2002). In Study 2, we carried out the same analysis plan as in Study 1

(preregistered at https://osf.io/sajxv/?view_only=58ead0c0dcc04508866e97fe0f795ab1),

in order to replicate associations of self-control and stable mental processing in an

already collected sample of $N=101$ participants (58 females). As a conceptual extension,

we tested the hypothesis that stable mental processing is negatively associated with risk-

taking behavior (BART; Lejuez et al., 2002).

**Results (Study 1)**

Descriptive Analyses

As expected, we found considerable heterogeneity of self-control across different measurement domains. Self-reported self-control as measured with the BSCS amounted to an average of 37.60 points (*SD*=6.90; range: 19-51) and the neural index of inhibitory control as measured by the average amplitude of the P300 during response inhibition amounted to an average of 5.73 µV (*SD*=2.23; range: 1.78-12.64). Self-reported self-control was not significantly associated with the neural index of inhibitory control (*r*=.11, 95% CI [-.16, .35], *p*=.431).

On average, there were 158.88 seconds of artefact-free resting-state EEG data available for microstate analyses (*SD*=31.39; range: 54.10-219.00). In close accordance with previous findings, the four prototypical microstate types accounted for an average of 77.87% of EEG signals (*SD*=3.26; range: 70.40-84.20). See Fig. 1 for grand-mean microstate maps and exemplary sequences of microstates for individuals with stable and unstable mental processing (see Table S1 in the supplemental materials for descriptive statistics of study 1). Supporting the assumption that people display a general tendency for more or less stable mental processing, durations (A*B: *r*=.58, 95% CI [.38, .73], *p*<.001; A*C: *r*=.59, 95% CI [.40, .74], *p*<.001; A*D: *r*=.60, 95% CI [.40, .74], *p*<.001; B*C: *r*=.64, 95% CI [.45, .77], *p*<.001; B*D: *r*=.59, 95% CI [.40, .74], *p*<.001; C*D: *r*=.58, 95% CI [.37, .73], *p*<.001) and occurrences (A*B: *r*=.59, 95% CI [.40, .74], *p*<.001; A*C: *r*=.39, 95% CI [.14, .59], *p*=.003; A*D: *r*=.39, 95% CI [.15, .59], *p*=.002; B*C: *r*=.57, 95% CI [.36, .72], *p*<.001; B*D: *r*=.45, 95% CI [.21, .63], *p*<.001; C*D: *r*=.54, 95% CI [.32, .70], *p*<.001) of all four microstate types showed considerable positive correlations. This confirms that the temporal stability of one microstate network naturally goes along with the temporal stability of all other microstate networks.

Adding a random intercept across participants to a model of microstate duration increased the model-fit ($p<.001$), confirming the need for linear mixed model analyses. Correspondingly, a high intra class correlation ($ICC=.600$) indicated that durations of the four microstate types were correlated, which again means that people tend to have higher or lower durations of microstates across microstate types. The same pattern applies for microstate occurrences (increase in model fit with $p<.001$; $ICC=.493$).

Figure 1

Grand-mean Microstate Maps in Study 1 and Exemplary Microstate Sequences
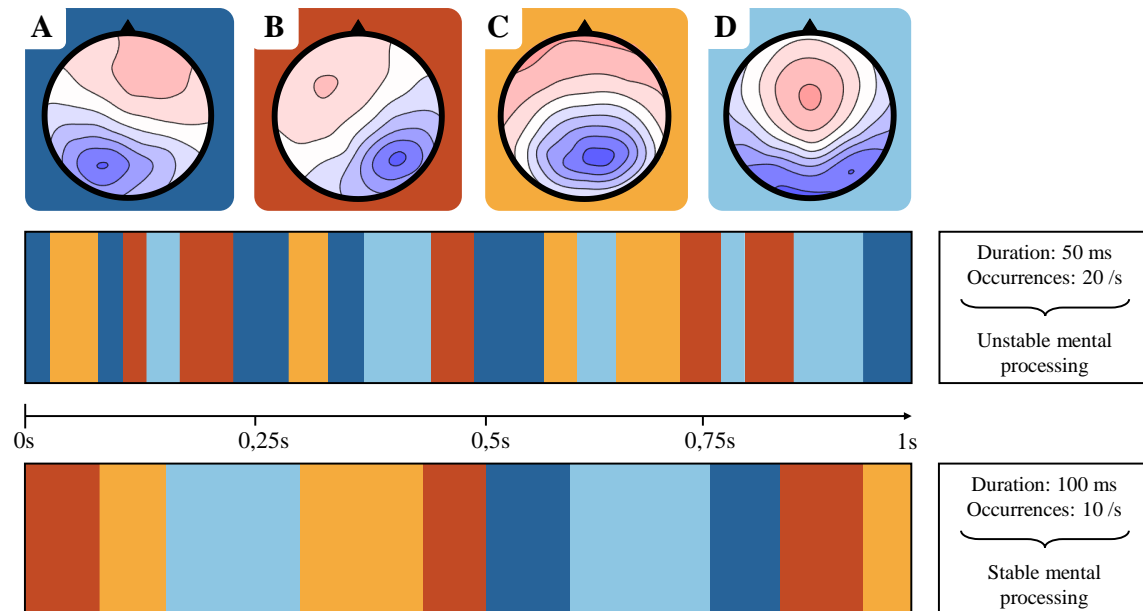
Note. Top: Grand-mean maps of resting-state microstates in Study 1. Note that the four empirically identified microstate maps closely resemble the prototypical microstate maps known from the literature (Michel & Koenig, 2018). Middle and bottom: Exemplary 1-second sequences of resting-state microstate networks for an individual with unstable mental processing (middle sequence) and an individual with stable mental processing (bottom sequence). Compared to the individual with unstable mental processing, the

individual with stable mental processing shows a longer average microstate duration

across network types (100ms vs 50ms) and less occurrences of microstates per second
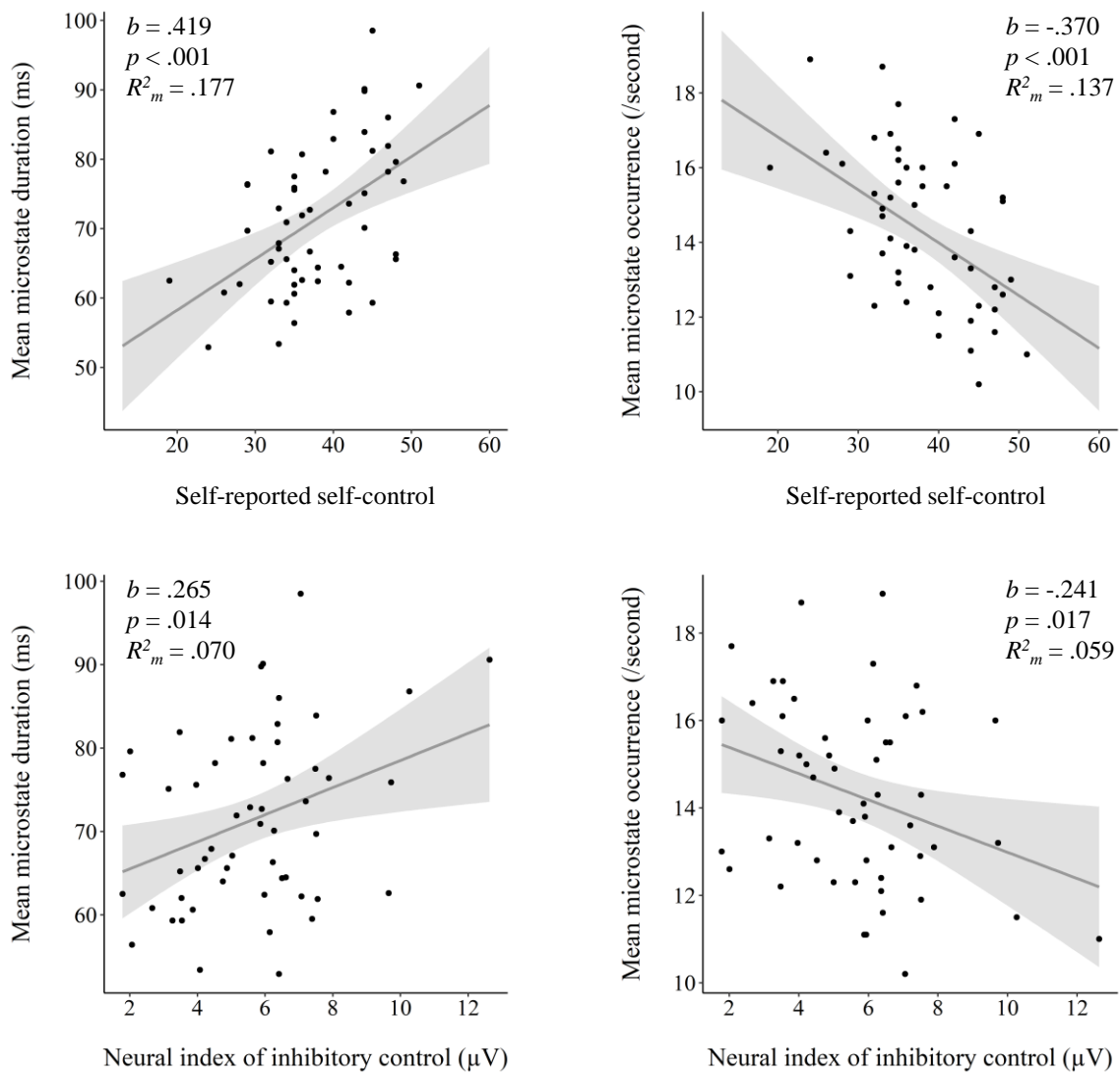
(10 vs 20).

Associations of Self-Reported Self-Control and Stable Mental Processing

As hypothesized, the duration of resting-state microstates was positively related to self-

reported self-control (b=.419, 95% CI [.230, .609], SE=.095, $t(56)$=4.41, p<.001,

R^2_m=.177; see Fig. 2). To test whether this effect was driven by specific microstate types,

we tested for an interaction of self-reported self-control with microstate types. We found

a significantly higher model-fit after including interactions with microstate types to the

model (p=.046), due to a weaker association of self-reported self-control with the

duration of type A compared to type B (p=.006). However, durations of all four

microstate types were positively associated with self-reported self-control, supporting our

assumption of a type-independent association of microstate network stability and self-

control (see Table S3 in the supplemental materials for correlations). Furthermore, the

occurrence of resting-state microstates was negatively related to self-reported self-control

(b=-.370, 95% CI [-.552, -.188], SE=.091, $t(56)$=-4.05, p<.001, R^2_m=.137; see Fig. 2).

Again, adding interactions with microstate types to the model resulted in a higher model-

fit (p=.012), revealing a stronger (negative) association of self-reported self-control with

the occurrence of type A compared to the types B (p=.002), C (p=.016) and D (p=.018).

However, occurrences of all four microstate types were negatively associated with self-

reported self-control, again demonstrating the type-independent association of microstate

network stability and self-control. Adding to the reliability of our findings, effects were

robust when controlling for EEG quality (see Table S4 in the supplemental materials) and

when removing outliers with regard to microstate characteristics (see Table S2 in the

supplemental materials). Taken together, these results suggest that self-controlled

individuals show a higher stability of mental processing in the brain when no task is at

hand.

Figure 2

Associations of Stable Mental Processing with Self-Reported Self-Control and a Neural

Index of Inhibitory Control

Note. Top left: Scatterplot illustrating the association of the mean microstate duration across the types A-D with self-reported self-control (BSCS; Tangney et al., 2004). Top right: Scatterplot illustrating the association of the mean microstate occurrence across the types A-D with self-control. Bottom left: Scatterplot illustrating the association of the mean microstate duration with the neural index inhibitory control as measured by the amount of electrical activity in the timeframe of the P300 (Global Field Power averaged over 300-423ms after stimulus onset) in the NoGo-condition of the CPT (Fallgatter et al., 1997). Bottom right: Scatterplot illustrating the association of the mean microstate occurrence with the neural index inhibitory control. All plots include 95% confidence intervals and coefficients resulting from mixed model analyses.

Associations of a Neural Index of Inhibitory Control and Stable Mental Processing

In a second set of analyses, we used a neural index of inhibitory control (amount of electrical activity in the timeframe of the NoGo P300; obtained from the CPT) to predict the duration of microstates in a mixed model. As expected, the neural index of inhibitory control was positively related to microstate duration (b=.265, 95% CI [.056, .473], SE=.104, $t(56)$=2.54, p=.014, R^2_m=.070; see Fig. 2). All microstate types contributed equally to this effect, as there was no increased model-fit testing for an interaction with microstate types (p=.166). Furthermore, the neural index of inhibitory control was negatively related to microstate occurrence (b=-.241, 95% CI [-.438, -.045], SE=.098, $t(56)$=-2.45, p=.017, R^2_m=.059, see Fig. 2), indicating that participants with fewer occurrences of microstates show an increased electrophysiological response inhibition capacity. Again, all microstate types contributed equally to this effect, as there was no increased model-fit testing for an interaction with microstate types (p=.096). These

findings suggest that an increased P300 response during response inhibition is associated with stable mental processing (see Fig. 2; see Table S3 in the supplemental materials for correlations; see Table S2 in the supplemental materials for outlier analyses demonstrating the robustness of these associations).

To test for their combined predictive power for stable mental processing, we used self-reported self-control and the neural index of inhibitory control as joint predictors for the duration (and occurrence) of microstates in multiple predictor linear mixed models. Both measures of self-control showed incremental validity on top of each other for the prediction of the duration (self-reported self-control: b=.396, 95% CI [.214, .578], SE=.091, t(55)=4.32, p<.001; neural index of inhibitory control: b=.223, 95% CI [.041, .404], SE=.091, t(55)=2.44, p=.018; R^2_m=.226) and the occurrence of microstates (self-reported self-control: b=-.348, 95% CI [-.523, -.173], SE=.088, t(55)=-3.96, p<.001; neural index of inhibitory control: b=-.205, 95% CI [-.380, -.030], SE=.088, t(55)=-2.33, p=.024; R^2_m=.179). Compared to single-predictor models only using self-reported self-control as a predictor, adding the neural index of inhibitory control increased the amount of variance explained in microstate duration by 4.6% (from 17.7% to 22.3%) and in microstate occurrence by 4.2% (from 13.7% to 17.9%). These results illustrate independent associations of stable mental processing with both perceptions and neural processes related to self-control.

Associations of Control-Related Brain Areas and Stable Mental Processing

We used sLORETA (Pascual-Marqui, 2002) to identify neural sources of inhibitory control during the CPT (i.e., voxels that were more active during the P300 in the NoGo-condition compared to the P300 in the Go-condition) that were associated with task-

independent stable mental processing. We identified a significant positive correlation of

current source density estimates originating from the left insula and inferior frontal gyrus

(GFP-channel, 14 voxels, $p<.05$, corrected; see Fig. 3 and Table S5 in the supplemental

materials) and the mean duration of microstates ($r=.42$, 95% CI [.187, .616], $p<.001$),

indicating that people with stronger activity in these regions during response inhibition

show more stable mental processing at rest (there were no significant associations with

the mean occurrence of microstates).

Figure 3

Association of Mean Microstate Duration with Source-Localized Brain Activity
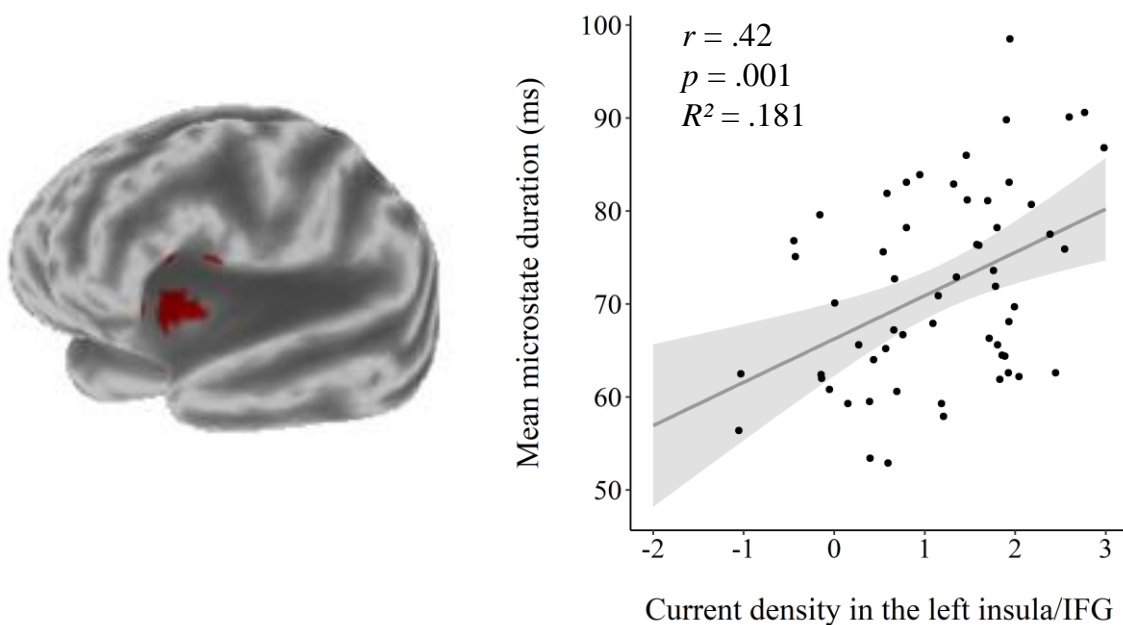
Note. Left: Locations of the voxels that showed significant correlations are indicated in

red (*corrected p<.05*). Right: Scatterplot illustrating the association of mean microstate

duration with current density (GFP-channel) in 14 voxels during the NoGo condition of

the CPT (demonstrating the average correlation across all voxels that exceeded the

corrected p-threshold in the same cluster). We found positive associations between

microstate duration and current density in the left insula (BA 13; 10 voxels; peak voxel at

MNI (x,y,z) -40, 15, 5), and in the left inferior frontal gyrus (IFG; BAs 44, 45, and 47; 4

voxels; peak voxel at MNI (x, y, z) –40, 15, 5).

Results (Study 2)

Descriptive Analyses

Again, we found high heterogeneity of self-control across different measurement

domains. Self-reported self-control as measured with the BSCS amounted to an average

of 39.12 points (SD=6.90; range: 18-59) and risk-taking behavior as measured by the

BART amounted to an average of 3.91 points (SD=2.73; range: 0.13-12.68). Self-

reported self-control was not significantly associated with risk-taking behavior (r=-.001,

95% CI [-.196, .195], p=.996).

On average, there were 105.64 seconds of artefact-free resting-state EEG data

available for microstate analyses (SD=9.30; range: 50.94-112.70), and the four

prototypical microstate types accounted for an average of 74.71% of EEG signals

(SD=4.78; range: 55.93-84.43; see Table S6 and S7 in the supplemental materials for

grand-mean microstate maps and detailed descriptive statistics of study 2).

Replication Analysis: Associations of Self-Reported Self-Control and Stable Mental Processing

As hypothesized via our preregistered analysis plan, a positive association of self-

reported self-control with microstate duration was replicated, albeit with a more modest

effect size than in study 1 (b=.179, 95% CI [.003, .354], SE=.089, t(99)=2.02, p=.046,

R^2_m=.032; see Fig. 4). To test whether this effect was driven by specific microstate types,

we tested for an interaction of self-reported self-control with microstate types. We did not

find a significantly higher model-fit after including interactions with microstate types to

the model (p=.090), illustrating that all microstate types contributed to the effect (see

Table S8 in the supplemental materials for correlations). In an analogous analysis, a

negative association of self-reported self-control with microstate occurrence was not

replicated (b=-.140, 95% CI [-.315, .035], SE=.088, $t(99)$=-1.59, p=.116, R^2_m=.020; see

Fig. 4). Critically, this association was significant (b=-.171, 95% CI [-.302, -.039],

SE=.066, $t(95)$=-2.57, p=.012, R^2_m=.052) after removing outliers with regard to

microstates characteristics (see Table S2 in the supplemental materials). Adding

interactions with microstate types to the model did not result in a higher model-fit

(p=.290). Overall, study 2 provided somewhat mixed evidence regarding the association

of self-reported self-control and stable mental processing compared to study 1. However,

outlier analyses support a replication of study 1's findings.

Figure 4

Associations of Stable Mental Processing with Self-Reported Self-Control and Risk-

Taking Behavior

Note. Top left: Scatterplot illustrating the association of the mean microstate duration

across the types A-D with self-reported self-control (BSCS; Tangney et al., 2004). Top

right: Scatterplot illustrating the association of the mean microstate occurrence across the

types A-D with self-control. Bottom left: Scatterplot illustrating the association of the

mean microstate duration with risk-taking behavior as measured in the BART (Lejuez et

al., 2002). Bottom right: Scatterplot illustrating the association of the mean microstate

occurrence with risk-taking behavior. All plots include 95% confidence intervals and

coefficients resulting from mixed model analyses.

Conceptual Extension: Associations of Risk-Taking Behavior and Stable Mental

Processing

As a conceptual extension, we tested for associations of stable mental processing with

risk-taking behavior. As hypothesized, risk-taking behavior was negatively related to

microstate duration (b=-.228, 95% CI [-.400, -.055], SE=.087, t(99)=-2.61, p=.010,

R^2_m=.052; see Fig. 4). There was no higher model-fit after including interactions with

microstate types to the model (p=.389). Furthermore, risk-taking behavior was positively

associated with microstate occurrence (b=.220, 95% CI [.049, .391], SE=.086,

t(99)=2.55, p=.012, R^2_m=.049; see Fig. 4), indicating that the positive association of the

temporal stability of resting EEG networks with risk-taking behavior is driven by both

the duration and the occurrence of microstates (see Table S8 in the supplemental

materials for correlations; see Table S2 in the supplemental materials for outlier analyses

demonstrating the robustness of these associations). Adding interactions with microstate

types to the model did not result in a higher model-fit (p=.156).

　　　　Next, we used self-reported self-control and risk-taking behavior as joint

predictors for the duration and occurrence of resting-state microstates in multiple

predictor linear mixed models. Both predictors showed incremental validity on top of

each other for the prediction of microstate duration (self-reported self-control: b=.179,

95% CI [.009, .348], SE=.086, t(98)=2.08, p=.040; risk-taking behavior: b=-.228, 95% CI

[-.397, -.059], *SE*=.085, *t*(98)=-2.67, *p*=.009 R^2_m=.084), and risk-taking behavior showed

incremental validity on top of self-reported self-control for the prediction of microstate

occurrence (self-reported self-control: *b*=-.140, 95% CI [-.309, .029], *SE*=.086,

t(98)=-1.64, *p*=.105; risk-taking behavior: *b*=.220, 95% CI [.051, .388], *SE*=.085,

t(98)=2.58, *p*=.012; R^2_m=.068). Compared to single-predictor models only using self-

reported self-control as a predictor, adding risk-taking behavior increased the amount of

variance explained in microstate duration by 5.2% (from 3.2% to 8.4%) and in microstate

occurrence by 4.9% (from 1.9% to 6.8%). These results illustrate independent

associations of stable mental processing with both perceptions and behavioral preferences

related to self-control.

Association of Self-Reported Self-Control and Stable Mental Processing Across

Both Studies

In a final set of analyses, we combined the samples of Study 1 and Study 2 (*N*=159) to

identify the overall association of stable mental processing with self-reported self-control.

Across samples, self-reported self-control was positively related to microstate duration

(*b*=.266, 95% CI [.135, .398], *t*(157)=3.99, *p*<.001, R^2_m=.071), and negatively related to

microstate occurrence (*b*=-.224, 95% CI [-.353, -.094], *t*(157)=3.40, *p*<.001, R^2_m=.050;

see Table S2 in the supplemental materials for outlier analyses demonstrating the

robustness of these associations). There were no interactions with microstate types

(prediction of microstate duration: *p*=.975; prediction of microstate occurrence: *p*=.774),

indicating that all four types A, B, C and D contributed equally to both effects

(correlations of self-reported self-control with the duration of type A: *r*=.265, 95% CI

[.114, .404], *p*<.001, type B: *r*=.283, 95% CI [.133, .420], *p*<.001; type C: *r*=.256,

95% CI [.104, .396], *p*=.001 and type D: *r*=.261, 95% CI [.110, .400], *p*=.001;

correlations of self-control with the occurrence of type A: *r*=-.266, 95% CI [-.405, -.115],

p<.001; type B: *r*=-.204, 95% CI [-.349, -.050], *p*=.010; type C: *r*=-.208, 95% CI

[-.352, -.054], *p*=.009 and type D: *r*=-.216, 95% CI [-.360, -.062], *p*=.006).

Controlling for the Frequency Content of the EEG Data

Following a reviewer's suggestion, we analyzed associations of the mean spectral EEG

power of the delta, theta, alpha and beta frequency band with microstate duration and the

three indices of self-control. As several EEG power values were associated with

microstate duration and self-control indices (see Table S9 in the supplemental materials

for details), we re-calculated our main analyses including EEG power values as

additional predictors. Across samples, the association of self-reported self-control with

microstate duration remained significant (*b*=.227, 95% CI [.099, .355], *SE*=.065,

t(153)=3.47, *p*<.001). In study 1, the association of the neural index of inhibitory control

with microstate duration remained significant (*b*=.225, 95% CI [.052, .397], *SE*=.087,

t(52)=2.57, *p*=.013). In study 2, the association of risk-taking behavior with microstate

duration remained significant (*b*= -.215, 95% CI [-.385, -.044], *SE*=.086, *t*(95)= -2.48,

p=.015).

Discussion

Self-control is commonly defined as the ability to inhibit impulses in order to achieve

long-term goals. However, recent research has challenged the assumption that self-

control is all about inhibition. Based on both a theoretical account of self-control and

recent research, we hypothesized that self-control is associated with stable mental

processing as indicated by fewer, but longer lasting mental processing steps. In order to

test this hypothesis, we assessed mental processing stability by means of resting EEG microstates analysis, allowing us to determine individual durations and occurrences of mental processing steps when no task is at hand. Across two laboratories and two independent samples, we found that stable mental processing was associated with self-report, neural and behavioral measures of self-control. Our first exploratory study demonstrated strong associations of stable mental processing with self-reported self-control and a neural measure of inhibitory control (N_1=58 males). Following a pre-registered analysis plan, our second study (N_2=101 [58 females]) replicated associations of stable mental processing with self-reported self-control, albeit the effect sizes were more modest than in study 1 and the association of microstate occurrence and self-reported self-control was only significant after removing outliers. As a conceptual extension, study 2 revealed inverse associations of stable mental processing with risk-taking behavior. These analyses add to the robustness of our findings, yet also suggest that the first study may have somewhat over-estimated the true effect size in the general population.

Our findings resonate with recent expansions of the concept of self-control beyond the inhibition of impulses (Fujita, 2011; Inzlicht et al., 2021). Self-control has been defined more broadly as the process of advancing abstract, distal motives (e.g., the desire to lose weight) over conflicting, concrete, and proximal motives (e.g., eating high-caloric food). Though impulse inhibition is one important means used to solve this conflict, there might be other effective ways to do so. For example, one can proactively regulate the availability of temptations or cognitively reappraise the experience of temptations. One could speculate that individuals with stable mental processing are more

efficient in achieving long-term goals, because they have more stable mental processes

with fewer interruptions by distracting impulses (see also research on an "implemental

mindset" which promotes goal achievement by reducing attention to task-irrelevant

stimuli without the need for conscious monitoring; Fujita, 2011). This idea fits with

recent work suggesting that the biggest problem in goal achievement is not lacking

control to resolve conflict, but rather the presence of conflicting motives to begin with

(Inzlicht et al., 2021). Thus, people high in self-control may simply experience fewer

interrupting impulses rather than only being better at inhibiting them. Indeed, recent

research has observed less real-time conflict in individuals who are more successful at

self-control (Stillman et al., 2017).

Alongside the conceptual debate on the nature of self-control, there is an ongoing

discussion on how to best measure this construct. Recent meta-analytic evidence

demonstrates that different self-control measures often fail to correlate with each other

(Wennerhold et al., 2020). In line with this, self-reported self-control was not

significantly correlated with neural or behavioral self-control measures in our study.

Conversely, the temporal stability of resting EEG microstates was significantly

associated with self-report, neural and behavioral self-control measures. Thus, stable

mental processing might represent a domain-general feature of self-control, capturing

common variance of existing self-control measures. Note that the low convergent validity

of existing self-control measures has been attributed to its task- and domain-specific

measurement approach (Wennerhold et al., 2020). In contrast, stable mental processing as

identified by resting EEG microstate analysis constitutes a task- and domain independent

measure, possibly contributing to its robust associations with various (domain-specific) self-control measures.

In sum, relying on EEG microstates analysis, we provide evidence that self-control is characterized by stable mental processing as indicated by fewer, but longer lasting mental processing steps at rest. This study demonstrates that analyzing the temporal dynamics of task-independent brain activity can inform behavioral and cognitive sciences on the nature of the human mind. It also raises questions ripe for future research. Do our findings hold in larger sample sizes with distinct characteristics or are they limited to college students? Do individuals notice their degree of stable mental processing? Can we learn to engage in stable mental processing? Do stable mental processes at rest relate to stable mental processes while executing self-control? Following up on these questions has the potential to shed light on why some are better than others in implementing self-control and living a healthier and happier life.

Open Practices Statement

Study 2's analysis plan was preregistered [https://osf.io/sajxv/]. Anonymized data of both studies and an analysis script including a codebook are available online [https://osf.io/sk3pw/].

Method (Study 1)

Participants

Based on an estimated medium effect size of associations between resting-state microstate characteristics and trait variables in similar research (Schiller, Kleinert, et al., 2020), 56 participants (α=.05, *power*=.85, *r*=.35) were needed to detect a significant effect. To account for potential dropouts, we recruited 61 healthy right-handed men, all

free of current or previous history of physical and psychiatric disorders, and alcohol or

drug abuse. Two participants were excluded due to technical problems during EEG

measurements and one participant due to random response patterns in the Go/NoGo

reaction-time task, resulting in a final sample size of N=58 for all analyses. The mean age

was 24.09 years (SD=4.28, range: 18-40). Both studies were reviewed and approved by

the Institutional Review Board of each university and carried out with the adequate

understanding and informed written consent of participants according to the principles

expressed in the Declaration of Helsinki.

Procedure

Exclusion criteria were assessed in an online screening questionnaire. Prior to the

experimental procedure, participants completed the BSCS (Tangney et al., 2004) online.

They then took part in two laboratory sessions, each run by two trained study assistants.

In the first session of 90 minutes, participants were seated in a darkened, electrically

shielded cabin for the recording of 64-channel resting EEG. A chin rest was used, and

subjects were instructed to move as little as possible to minimize artefacts. Resting-state

EEG was recorded for five minutes using a routine protocol consisting of 20-s eye open

periods followed by 40-s eyes closed periods, repeated five times (Schiller et al., 2014,

2019). This procedure is used in order to minimize fluctuations in vigilance states of

participants. Instructions were given via intercom. Next, participants completed the

Continuous Performance Test (CPT; Fallgatter et al., 1997) and other paradigms that are

not part of the current study. Participants also completed a second experimental session,

in which interactive paradigms were assessed that are evaluated elsewhere. On average,

participants received a monetary compensation of 45.18€ (SD=1.18; range: 43.50-48.10).

Measurement of Self-Reported Self-Control and a Neural Index of Inhibitory Control

We measured self-reported self-control using the BSCS (Tangney et al., 2004), including 13 items on different self-control-related domains (e.g., "I am good at resisting temptation"). For each item, participants indicate how much it reflects how they typically are on a 5-point Likert scale (1="not at all" to 5="very much"), resulting in a final score of 13-65 points. The BSCS shows good internal consistency (α=.83-.85) and test-retest-reliability after 3 weeks (r=.87), and predicts a wide range of health-related and social outcomes (Tangney et al., 2004). Additionally, we used the *Continuous Performance Test* (CPT) as a standard procedure to assess response inhibition using electrophysiological data (Fallgatter et al., 1997). The task for participants was to press a response button, if an "O" is followed by an "X" (O $\rightarrow$ X; Go-condition; 40 stimuli) in a series of 400 letters that appeared on screen for 200ms with an inter-stimulus interval of 1650ms. Response inhibition is required if an "O" is not followed by an "X" (e.g., O $\rightarrow$ F; NoGo-condition; 40 stimuli). Other letters are either primers (O; 80 stimuli) or distractors (e.g., B; 240 stimuli). A neural index of inhibitory control was calculated as the baseline-corrected, average event-related P300 response in NoGo-trials in a timeframe of coordinated mental activity in the brain (for details, see event-related EEG analysis).

EEG Recording and Preprocessing

Continuous resting-state EEG was recorded in an electrically shielded cabin with a sampling rate of 1000Hz and an online band-pass filter between 0.1 and 100Hz using 64 Ag-AgCI active electrodes (actiCAP; Brain Products GmbH, Munich) arranged in the extended 10-20 system on the scalp. The signal was referenced online to an electrode on

site FCz, the grounding electrode was placed at AFz. Electrooculographic signals were

measured by two electrodes at the left and right outer canthi (horizontal movement) and

the left infra- and supraorbital (vertical movement). Preprocessing of all EEG data was

conducted in the Brain Vision Analyzer (version 2.1.0.327; Brain Products GmbH,

Munich). A notch filter of 50Hz and an additional band-pass filter of 2 to 20Hz were

applied on resting-state EEG data (Michel & Koenig, 2018) and an additional band-pass

filter of 0.1 to 30Hz in case of event-related EEG data (Schiller et al., 2016). Eye

movement artefacts were removed using a semi-automatic independent component

analysis. EEG channels heavily affected by artefacts were interpolated using neighboring

electrodes. Remaining artefacts were automatically identified first (maximum amplitude

$\pm$ 100µV) and corrected manually to eliminate remaining artefacts. Finally, the signal was

re-derived to average reference.

EEG Resting-State Microstate Analysis

To obtain individual information on the temporal stability of microstate networks at rest

(i.e., stable mental processing), microstate analyses were conducted in EEGLAB

(Delorme & Makeig, 2004) using a plugin for resting-state microstate analyses by Koenig

(2017) that works according to standard procedures (Pascual-Marqui et al., 1995). First,

resting EEG signals were down-sampled to 500Hz and split into segments of two seconds

(Khanna et al., 2014). Second, EEG-data from all channels (electric potential field maps)

were extracted at time points of maximum global field power (GFP), ensuring optimal

signal-to-noise ratio (Michel & Koenig, 2018), and submitted to an atomize-agglomerate

hierarchical clustering procedure (AAHC) for the identification of the four most

predominant microstate-maps in each subject (Murray et al., 2008). In line with the

literature, the polarity of maps was ignored as inverted polarities emerge from

oscillations of the same underlying electrical source generators (Michel & Koenig, 2018).

Third, maps of all subjects were included in a second cluster analysis to obtain grand-

mean microstate maps, which were manually sorted to fit the standard order (Michel &

Koenig, 2018). Grand-mean microstate maps of our data closely resemble the four

prototypical resting-state microstate types A, B, C and D known from the literature (see

Fig. 1; Michel & Koenig, 2018). Next, individual microstate maps were assigned to one

of the four grand-mean microstate maps according to spatial correlations. Finally,

individual maps from GFP peaks were assigned to the best fitting predominant

microstate-map, resulting in a continuous temporal series of microstates for each subject

from which we extracted the average duration of each microstate type in milliseconds and

the average number of occurrences of each microstate type per second. As we were

interested in the general, type independent temporal stability of resting-state microstates,

duration refers to the duration of all four microstate types, and *occurrence* refers to the

number of occurrences of all four microstate types per second. Overall, *stable mental*

processing is reflected by longer durations and fewer occurrences of microstates across

microstate types (as longer durations naturally go along with fewer occurrences).

EEG Event-Related Analysis

To obtain a neural index of inhibitory control, we first identified event-related potentials

(ERPs) in response to the Go- and NoGo-condition in the Continuous Performance Test

(CPT; timeframe of -200 to 1000ms after stimulus presentation). ERPs were baseline-

corrected (baseline: -200 to 0ms after stimulus presentation) and averaged. A topographic

consistency test (Koenig et al., 2011) showed that there was no communality in EEG

signals across subjects earlier than 50ms after stimulus onset, which is why we chose a

timeframe of 50 to 1000ms after stimulus presentation for further analyses. Next, we used

an event-related microstate analysis (e.g., Schiller et al., 2016) to identify sequences of

microstate networks in response to the Go and NoGo-condition of the CPT. For this

purpose, ERPs were submitted to a modified k-means clustering procedure (300 random

trials; minimum length of 30ms; conserving the polarity of the maps) in the software

CARTOOL, using global map dissimilarity as an index of topographic difference

between maps to identify the most dominant topographic networks (Brunet et al., 2011).

Then, we generated grand-mean sequences of these networks in a newly generated

channel of global field power (GFP) for the Go- and the NoGo-condition using a

topographic fitting procedure. The ideal number of 7 microstate networks was identified

via a synthetic meta-criterion for the best fitting microstate solution provided by

CARTOOL (Custo et al., 2017; Michel & Koenig, 2018). In line with previous research,

we found a prolonged latency of the P300 peak and a more anterior activation in the

NoGo-condition compared to the Go-condition (Fallgatter et al., 1997). Notably, we

identified an additional, more anterior microstate network in the NoGo-condition in a

timeframe of 300 to 423ms after stimulus presentation, which was not existent in the Go-

condition (which is evaluated in detail elsewhere). A neural index of inhibitory control

was calculated as the baseline-corrected, average amount of electrical activity (i.e.,

Global Field Power) in this timeframe of coordinated mental activity following response

inhibition.

EEG Source Localization Analysis

The sLORETA (Pascual-Marqui, 2002) solution space, which has been used in many

EEG studies (e.g., Leota et al., 2021; Nash et al., 2013; Schiller, Domes, et al., 2020;

Schiller et al., 2014), consists of 6.239 voxels (voxel size: $5 \times 5 \times 5$ mm) and is restricted

to cortical grey matter and hippocampi, as defined by the digitized Montreal Neurological

Institute probability atlas. The sLORETA functional images represent the estimated

electrical activity at each voxel as squared magnitude (i.e., power) of computed current

density (unit: amperes per square meter, A/m^2). sLORETA estimates the electrical

neuronal activity without assuming a predefined number of sources. Our aim was to

identify the intracerebral sources underlying the association of the NoGo P300 and stable

mental processing. For that purpose, we averaged all scalp maps within the time periods

covered by the P300-microstate in the Go- and NoGo conditions of the CPT (i.e., 300-

423ms after stimulus onset; fixed time window across participants) and then estimated

the individual sLORETA images. Using the regularization method in the sLORETA

software, we chose the transformation matrix with the signal-to-noise set to 10. To reduce

confounds that have no regional specificity, we normalized sLORETA images for each

subject and for each condition to a total power of one and then log-transformed them

before statistical analyses.

Statistical Analysis

The goal of the current study was to evaluate associations of self-control measures (self-

reported self-control and a neural index of inhibitory control) with stable mental

processing (i.e., longer durations and fewer occurrences of microstate networks). We

calculated two-tailed linear mixed models with microstate characteristics (i.e., duration,

occurrence) as dependent variables, self-control measures as independent variables, and

random intercepts across participants (no random slope used; see also Atluri et al., 2018).

To test, if characteristics of specific microstate types (A, B, C or D) show stronger or

weaker associations with indices of self-control, we added interactions with dummy

variables of microstate types to the respective model in a next step, allowing for a direct

comparison of effects between microstate types (see Table S10 in the supplemental

materials for a full exemplary analysis). All metric variables were z-standardized prior to

analyses. Marginal R-squared values (R^2_m) were calculated following the recommended

procedure by Nakagawa and Schielzeth (2013). In a first set of analyses, we tested for

associations of self-reported self-control with the duration and occurrence of resting-state

microstates using the procedure described above. In a second set of analogous analyses,

we tested for associations of a neural index of inhibitory control with the duration and

occurrence of microstates. Next, we added both indices of self-control as joint predictors

in one linear mixed model to test if a higher percentage of variance in the duration (and

occurrence) of resting-state microstates can be explained by combining self-report and

neural measures of self-control. To test for the reliability of our results, we repeated the

main analyses using microstate characteristics adjusted for the total EEG time available

in order to control for EEG quality (see Table S4 in the supplemental materials).

Furthermore, we found associations of the mean spectral EEG power of the delta, theta,

alpha and beta frequency band with microstate duration and self-control indices (see

Table S9 in the supplemental materials). Therefore, we controlled for power values by

adding them as additional predictors to our main analyses. We also tested for the

robustness of our findings by excluding outliers with regard to microstate characteristics

(see Table S2 in the supplemental materials). All analyses yielded highly comparable

results. Lastly, we examined whether source-localized brain activity during response

inhibition in the CPT was associated with the temporal stability of resting-state

microstates by regressing the sLORETA images of the NoGo condition on the average

duration of resting-state microstates. We restricted this voxel-by-voxel regression

analysis to voxels, which were more active during the NoGo- compared to the Go-

condition (461 voxels encompassing mostly fronto-cingulate regions; $p<.01$; see Table S5

in the supplemental materials). Correction for multiple testing was implemented by

means of a nonparametric randomization approach, which estimated the empirical

probability distributions and the corresponding corrected (for multiple comparisons)

critical probability thresholds ($r>.37$, $p<.05$).

Method (Study 2)

Participants

For a preregistered replication analysis in Study 2, we used an already collected,

substantially larger sample of 110 first year psychology students. Nine participants were

excluded due to poor quality of resting EEG recordings, resulting in a final sample size of

$N=101$ for all analyses (58 females, 43 males). The mean age was 19.76 years ($SD=1.62$,

range: 17-26). Gender differences were not further considered in Study 2, as females and

males did not show any significant differences (see Table S11 in the supplemental

materials).

Procedure

Participants were equipped with a 64-channel EEG system (Brain Products GmbH,

Munich, Germany). All tasks were completed in an electrically- and noise-shielded cabin

on a computer using Presentation (version 18.0, Neurobehavioral Systems, Inc.,

Berkeley, CA). First, demographic information and several questionnaires were collected,

including the BSCS. Second, a four-minute resting EEG was recorded (60-s eyes-open

period followed by a 60-s eyes-closed period, repeated two times in total). Again, only

eyes-closed periods were used for further EEG analysis (two minutes). Participants were

then randomly assigned to one of two experimental conditions that are unrelated to the

current study (anxiety or control). Note that controlling for experimental conditions had

no impact on the main results of this study (see Table S12 in the supplemental materials).

Afterwards, participants completed two tasks that will be evaluated elsewhere, followed

by the BART for the measurement of risk-taking behavior. Finally, participants were

thanked for their time and compensated with class credit. The average duration of the

experiment was 110 minutes.

Measurement of Self-Reported Self-Control and Risk-Taking Behavior

Self-reported self-control was measured with the BSCS that we used in Study 1 (Tangney

et al., 2004). Risk-taking behavior was measured with the BART, which is associated

with self-control deficiencies, impulsivity and sensation seeking, as well as addictive,

safety- and health-risk behavior (Lejuez et al., 2002). In the BART, participants were

informed that they could increase their number of ballots in a lottery (price of 100$) by

performing well in a balloon-pumping game. The task was to press a button to pump up

balloons (20 in total) that would explode after an unknown and variable number of pumps

(explosion threshold; 15 pumps on average). Balloons were inflated more and more with

every pump, each earning one ballot but also bringing the balloon closer to the explosion

threshold. Participants earned no ballots for exploded balloons. In each trial, they could

stop pumping at any time in order to retain the earned ballots and continue with the next

trial. An individual score of risk-taking behavior (RT) was computed as (RT=average

pumps * (explosions + 1)/total number of trials). Thus, RT increases with a higher

average number of pumps and explosions, making it a more sensitive and valid measure

of risk-taking compared to traditional measures which focus on the number of either

pumps or explosions (also see Leota et al., 2021). Following a reviewer's suggestion, we

also checked whether our findings remain robust when using an alternative risk-taking

score, as originally proposed by Lejuez et al., 2002. All reported associations remained

significant (association of the alternative risk-taking measure with microstate duration:

b=-.215, 95% CI [-.388, -.042], SE=.088, $t(99)$=-2.45, p=.016, R^2_m=.047; association of

the alternative risk-taking measure with microstate occurrence: b=.198, 95% CI [.026,

.370], SE=.087, $t(99)$=2.28, p=.025, R^2_m=.040).

EEG Recording, Preprocessing and Resting-State Microstate Analysis

In our Canadian sample, continuous resting-state EEG was recorded in an electrically

shielded cabin with a sampling rate of 500Hz and an online band-pass filter between 0.1

and 100Hz using 64 Ag-AgCI active electrodes (actiCHamp; Brain Products GmbH,

Munich) arranged in the 10-10 system on the scalp. The signal was referenced online to

an electrode on site TP9 over the left mastoid. EEG preprocessing-steps and the resting-

state microstate analysis were conducted in the exact same way as in Study 1.

Statistical Analysis

Again, we calculated linear mixed models with microstate characteristics (i.e., duration,

occurrence) as dependent variables, self-control and/or risk-taking behavior as

independent variables (all variables z-standardized), and a random intercept across

participants (no random slope used). Again, we added interaction-terms with dummy

variables of microstate types to the respective model in a next step, allowing for a direct comparison of effects between microstate types. First, we aimed to replicate a positive association of self-reported self-control with microstate duration and a negative association with microstate occurrence. Second, we applied a conceptual extension by testing for a negative association of risk-taking behavior with microstate duration and a positive association with microstate occurrence. Finally, we added both self-reported self-control and risk-taking behavior as joint predictors in multiple predictor linear mixed models to test if a higher percentage of variance in the duration (and occurrence) of resting-state microstates can be explained by combining self-report and behavioral measures of self-control.

Acknowledgments

Competing Interests Statement: The authors declare that they have no competing interests.

References

Atluri, S., Wong, W., Moreno, S., Blumberger, D. M., Daskalakis, Z. J., & Farzan, F.

(2018). Selective modulation of brain network dynamics by seizure therapy in

treatment-resistant depression. *NeuroImage: Clinical*, *20*, 1176–1190.

Baumeister, R. F., Vohs, K. D., & Tice, D. M. (2007). The strength model of self-control.

Current Directions in Psychological Science, *16*(6), 351–355.

Bréchet, L., Brunet, D., Perogamvros, L., Tononi, G., & Michel, C. M. (2020). EEG

microstates of dreams. *Scientific Reports*, *10*(1), 1–9.

Brunet, D., Murray, M. M., & Michel, C. M. (2011). Spatiotemporal analysis of

multichannel EEG: CARTOOL. *Computational Intelligence and Neuroscience*,

2011, 2.

Castellanos, F. X., Sonuga-Barke, E. J., Milham, M. P., & Tannock, R. (2006).

Characterizing cognition in ADHD: Beyond executive dysfunction. *Trends in

Cognitive Sciences*, *10*(3), 117–123.

Custo, A., Van De Ville, D., Wells, W. M., Tomescu, M. I., Brunet, D., & Michel, C. M.

(2017). Electroencephalographic Resting-State Networks: Source Localization of

Microstates. *Brain Connectivity*, *7*(10), 671–682.

https://doi.org/10.1089/brain.2016.0476

da Cruz, J. R., Favrod, O., Roinishvili, M., Chkonia, E., Brand, A., Mohr, C., Figueiredo,

P., & Herzog, M. H. (2020). EEG microstates are a candidate endophenotype for

schizophrenia. *Nature Communications*, *11*(1), 1–11.

De Ridder, D. T., Lensvelt-Mulders, G., Finkenauer, C., Stok, F. M., & Baumeister, R. F.

(2012). Taking stock of self-control: A meta-analysis of how trait self-control

relates to a wide range of behaviors. *Personality and Social Psychology Review*, *16*(1), 76–99.

Delorme, A., & Makeig, S. (2004). EEGLAB: An open source toolbox for analysis of single-trial EEG dynamics including independent component analysis. *Journal of Neuroscience Methods*, *134*(1), 9–21.

Deng, Y., Zhang, B., Zheng, X., Liu, Y., Wang, X., & Zhou, C. (2019). The role of mindfulness and self-control in the relationship between mind-wandering and metacognition. *Personality and Individual Differences*, *141*, 51–56.

Epstein, J. N., Erkanli, A., Conners, C. K., Klaric, J., Costello, J. E., & Angold, A. (2003). Relations between continuous performance test performance measures and ADHD behaviors. *Journal of Abnormal Child Psychology*, *31*(5), 543–554.

Fallgatter, A. J., Brandeis, D., & Strik, W. K. (1997). A robust assessment of the NoGo-anteriorisation of P300 microstates in a cued Continuous Performance Test. *Brain Topography*, *9*(4), 295–302.

Fassbender, C., Zhang, H., Buzy, W. M., Cortes, C. R., Mizuiri, D., Beckett, L., & Schweitzer, J. B. (2009). A lack of default network suppression is linked to increased distractibility in ADHD. *Brain Research*, *1273*, 114–128.

Fujita, K. (2011). On conceptualizing self-control as more than the effortful inhibition of impulses. *Personality and Social Psychology Review*, *15*(4), 352–366.

Humphreys, K. L., & Lee, S. S. (2011). Risk taking and sensitivity to punishment in children with ADHD, ODD, ADHD+ ODD, and controls. *Journal of Psychopathology and Behavioral Assessment*, *33*(3), 299–307.

Inzlicht, M., Werner, K. M., Briskin, J. L., & Roberts, B. W. (2021). Integrating models

      of self-regulation. *Annual Review of Psychology*, *72*, 319–345.

Khanna, A., Pascual-Leone, A., & Farzan, F. (2014). Reliability of Resting-State

      Microstate Features in Electroencephalography. *PLOS ONE*, *9*(12), e114163.

      https://doi.org/10.1371/journal.pone.0114163

Koenig, T. (2017). *EEGLAB microstate plugin*. Microstates in EEGLAB.

      https://www.thomaskoenig.ch/index.php/software/microstates-in-eeglab/getting-

      started

Koenig, T., Kottlow, M., Stein, M., & Melie-García, L. (2011). Ragu: A free tool for the

      analysis of EEG and MEG event-related scalp field data using global

      randomization statistics. *Computational Intelligence and Neuroscience*, *2011*, 4.

Lehmann, D., Ozaki, H., & Pal, I. (1987). EEG alpha map series: Brain micro-states by

      space-oriented adaptive segmentation. *Electroencephalography and Clinical

      Neurophysiology*, *67*(3), 271–288. https://doi.org/10.1016/0013-4694(87)90025-3

Lejuez, C. W., Read, J. P., Kahler, C. W., Richards, J. B., Ramsey, S. E., Stuart, G. L.,

      Strong, D. R., & Brown, R. A. (2002). Evaluation of a behavioral measure of risk

      taking: The Balloon Analogue Risk Task (BART). *Journal of Experimental

      Psychology: Applied*, *8*(2), 75.

Leota, J., Kleinert, T., Tran, A., & Nash, K. (2021). Neural signatures of heterogeneity in

      risk-taking and strategic consistency. *European Journal of Neuroscience*, *54*(9),

      7214–7230.

Michel, C. M., & Koenig, T. (2018). EEG microstates as a tool for studying the temporal

    dynamics of whole-brain neuronal networks: A review. *NeuroImage*, *180*, 577–

    593. https://doi.org/10.1016/j.neuroimage.2017.11.062

Murray, M. M., Brunet, D., & Michel, C. M. (2008). Topographic ERP analyses: A step-

    by-step tutorial review. *Brain Topography*, *20*(4), 249–264.

Nagabhushan Kalburgi, S., Whitten, A. P., Key, A. P., & Bodfish, J. W. (2020). Children

    with autism produce a unique pattern of EEG microstates during an eyes closed

    resting-state condition. *Frontiers in Human Neuroscience*, 288.

Nakagawa, S., & Schielzeth, H. (2013). A general and simple method for obtaining R2

    from generalized linear mixed-effects models. *Methods in Ecology and Evolution*,

    4(2), 133–142. https://doi.org/10.1111/j.2041-210x.2012.00261.x

Nash, K., Schiller, B., Gianotti, L. R. R., Baumgartner, T., & Knoch, D. (2013).

    Electrophysiological Indices of Response Inhibition in a Go/NoGo Task Predict

    Self-Control in a Social Context. *PLOS ONE*, *8*(11), e79462.

    https://doi.org/10.1371/journal.pone.0079462

Pascual-Marqui, R. D. (2002). Standardized low-resolution brain electromagnetic

    tomography (sLORETA): Technical details. *Methods and Findings in*

    Experimental and Clinical Pharmacology, *24 Suppl D*, 5–12.

Pascual-Marqui, R. D., Michel, C. M., & Lehmann, D. (1995). Segmentation of brain

    electrical activity into microstates: Model estimation and validation. *IEEE*

    Transactions on Biomedical Engineering, *42*(7), 658–665.

Schiffer, A.-M., Waszak, F., & Yeung, N. (2015). The role of prediction and outcomes in

    adaptive cognitive control. *Journal of Physiology-Paris*, *109*(1–3), 38–52.

Schiller, B., Domes, G., & Heinrichs, M. (2020). Oxytocin changes behavior and spatio-
temporal brain dynamics underlying inter-group conflict in humans. *European
Neuropsychopharmacology*, *31*, 119–130.

Schiller, B., Gianotti, L. R. R., Baumgartner, T., & Knoch, D. (2019). Theta resting EEG
in the right TPJ is associated with individual differences in implicit intergroup
bias. *Social Cognitive and Affective Neuroscience*, *14*(3), 281–289.

Schiller, B., Gianotti, L. R. R., Baumgartner, T., Nash, K., Koenig, T., & Knoch, D.
(2016). Clocking the social mind by identifying mental processes in the IAT with
electrical neuroimaging. *Proceedings of the National Academy of Sciences*,
113(10), 2786–2791.

Schiller, B., Gianotti, L. R. R., Nash, K., & Knoch, D. (2014). Individual Differences in
Inhibitory Control—Relationship Between Baseline Activation in Lateral PFC
and an Electrophysiological Index of Response Inhibition. *Cerebral Cortex*,
24(9), 2430–2435. https://doi.org/10.1093/cercor/bht095

Schiller, B., Kleinert, T., Teige-Mocigemba, S., Klauer, K. C., & Heinrichs, M. (2020).
Temporal dynamics of resting EEG networks are associated with prosociality.
Scientific Reports, *10*(1), 13066. https://doi.org/10.1038/s41598-020-69999-5

Schiller, D., & Delgado, M. R. (2010). Overlapping neural systems mediating extinction,
reversal and regulation of fear. *Trends in Cognitive Sciences*, *14*(6), 268–276.

Stillman, P. E., Medvedev, D., & Ferguson, M. J. (2017). Resisting temptation: Tracking
how self-control conflicts are successfully resolved in real time. *Psychological
Science*, *28*(9), 1240–1258.

Tangney, J. P., Baumeister, R. F., & Boone, A. L. (2004). High self-control predicts good
    adjustment, less pathology, better grades, and interpersonal success. *Journal of
    Personality*, *72*(2), 271–324.

Vohs, K., Schmeichel, B., Lohmann, S., Gronau, Q. F., Finley, A. J., Wagenmakers, E.-
    J., & Albarracín, D. (2021). A multi-site preregistered paradigmatic test of the ego
    depletion effect. *Psychological Science*, *32*(10), 1566–1581.

Wennerhold, L., Friese, M., & Vazire, S. (2020). Why self-report measures of self-
    control and inhibition tasks do not substantially correlate. *Collabra: Psychology*,
    6(1).

Supplemental Materials

Table S1

Descriptive Statistics of all Variables in Study 1

Variable	Min	Max	Mean	SD
Measures of self-control				
Self-reported self-control (BSCS)	19	51	37.60	6.90
Neural index of inhibitory control (NoGo P300)	1.78	12.64	5.73	2.23
Microstate characteristics				
Duration network A	53.60	114.00	75.11	13.72
Duration network B	50.40	103.00	69.04	11.03
Duration network C	49.40	91.10	69.66	10.79
Duration network D	48.40	117.00	69.70	12.99
Mean duration A-D	52.90	98.50	71.60	10.42
Occurrence network A	2.53	5.22	3.77	.632
Occurrence network B	2.10	5.12	3.38	.692
Occurrence network C	2.15	5.43	3.50	.625
Occurrence network D	2.24	5.14	3.60	.661
Mean occurrence A-D	10.20	18.90	14.25	2.05

Note. $N = 58$. Min = minimum value, Max = maximum value, Mean = mean value, SD = standard deviation.

Table S2

Main Results Controlling for Outliers in Microstate Characteristics

Study 1 & 2: Predicting stable mental processing with self-reported self-control ($N = 152$; three outliers in microstate duration and five outliers in microstate occurrence removed)					
Microstate characteristics	*b*	*SDE*	*t(150)*	*p*	$R^2{}_m$
Duration	.265	.063	4.22	< .001	.080
Occurrence	-.220	.053	-4.16	< .001	.072

Study 1: Predicting stable mental processing with self-reported self-control ($N = 55$; two outliers in microstate duration and one outlier in microstate occurrence removed)					
Microstate characteristics	*b*	*SDE*	*t(54)*	*p*	$R^2{}_m$
Duration	.374	.094	3.97	< .001	.156
Occurrence	-.333	.091	-3.65	< .001	.120

Study 1: Predicting stable mental processing with the neural index of inhibitory control ($N = 55$; two outliers in microstate duration and one outlier in microstate occurrence removed)					
Microstate characteristics	*b*	*SDE*	*t(52)*	*p*	$R^2{}_m$
Duration	.259	.099	2.61	.012	.078
Occurrence	-.240	.094	-2.54	.014	.065

Study 2: Predicting stable mental processing with self-reported self-control ($N = 97$; four outliers in microstate occurrence removed)					
Microstate characteristics	*b*	*SDE*	*t(95)*	*p*	$R^2{}_m$
Duration	.197	.081	2.43	.017	.046

THE SELF-CONTROLLED MIND

	b	SDE	t(95)	p	$R^2{}_m$
Occurrence	-.171	.066	-2.57	.012	.052

Study 2: Predicting stable mental processing with risk-taking behavior ($N = 97$; four outliers in microstate occurrence removed)

Microstate characteristics	*b*	*SDE*	*t(95)*	*p*	$R^2{}_m$
Duration	-.184	.083	-2.21	.030	.038
Occurrence	.157	.068	2.29	.024	.042

Note. b = regression coefficient, SDE = standard error, t(df) = t-value (degrees of freedom), p = p-value, $R^2{}_m$ = marginal R-squared value. Results of mixed model analyses testing for the robustness of our findings when removing outlier values in microstate characteristics (+/- 3 standard deviations from the mean).

Table S3

Correlations of Study 1

Microstate characteristics	Self-reported self-control		Neural index of inhibitory control	
	r	*p*	*r*	*p*
Duration microstate A	.237	.074	.347	.008
Duration microstate B	**.559**	**< .001**	.113	.399
Duration microstate C	**.460**	**< .001**	**.336**	**.010**
Duration microstate D	**.422**	**.001**	**.263**	**.046**
Mean duration A-D	**.478**	**< .001**	**.330**	**.011**
Occurrence microstate A	**-.628**	**< .001**	-.185	.165
Occurrence microstate B	-.224	.091	**-.441**	**.001**
Occurrence microstate C	**-.311**	**.017**	-.139	.300
Occurrence microstate D	**-.316**	**.016**	-.201	.129
Mean occurrence A-D	**-.463**	**< .001**	**-.312**	**.017**

Note. N = 58. r = Pearson correlation coefficient; p = p-value. Bold values indicate

significant correlations (two-sided, alpha level = .05). Note that 8/8 correlations of

microstate durations with self-reported self-control and the neural index of inhibitory

control are positive, and 8/8 correlations of microstate occurrences with self-reported

self-control and the neural index of inhibitory control are negative.

Table S4

Main Effects Using Resting-State Microstate Characteristics Adjusted for the Total EEG

Time Available in Study 1

Predicting stable mental processing with self-reported self-control					
Microstate characteristics	*b*	*SDE*	*t(56)*	*p*	$R^2{}_m$
Duration (adjusted model 1)	.384	.098	3.92	< .001	.147
Occurrence (adjusted model 2)	-.344	.093	-3.69	< .001	.118
Predicting stable mental processing with the neural index of inhibitory control					
Microstate characteristics	*b*	*SDE*	*t(56)*	*p*	$R^2{}_m$
Duration (adjusted model 3)	.253	.105	2.41	.019	.064
Occurrence (adjusted model 4)	-.233	.099	-2.35	.022	.054

Note. N = 58. b = regression coefficient, t(df) = t-value (degrees of freedom), p = p-value, $R^2{}_m$ = marginal R-squared value. Participants with higher self-reported self-control might move less during resting EEG measures, resulting in a higher quality of the EEG signal and thus a higher duration (and a lower occurrence) of microstates. Addressing this issue, we calculated mixed model analyses using microstate characteristics adjusted for the total EEG time available as dependent variables. The total EEG time represents a strong indicator of EEG quality (i.e., more EEG time reflects higher quality), as artefacts were excluded from the signal (see method). Confirming our key findings (see Table 2, Figure 1, Figure 2), self-reported self-control and the neural index of inhibitory control (P300 activity in the NoGo-condition of the CPT) were positively associated with the adjusted duration, and negatively associated with the adjusted occurrence of microstates across all four types A-D. Testing for interactions with microstate types, we found an increased

model-fit ($p = .046$) in adjusted model 1 due to a lower association of self-reported self-control with the duration of type A compared to type B ($p = .006$) and an increased model-fit ($p = .012$) in adjusted model 2 due to a lower association of self-reported self-control with the occurrence of type A compared to the types B ($p = .002$), C ($p = .016$) and D ($p = .018$). Testing for interactions in the adjusted models 3 and 4, we did not find increased model-fits (all $p \geq .096$). In sum, these results confirm positive associations of both indices of self-control with microstate stability when controlling for total EEG time.

Table S5

Activated Voxels in the NoGo-Condition Compared to the Go-Condition in Study 1

Region	Hemisphere	BA	tmax	x	y	z	Voxels
Superior Frontal Gyrus	L/R	8/9	8.28	-20	40	50	35
Precentral Gyrus	L	4/6/9/43/44	8.07	-35	0	30	78
Middle Frontal Gyrus	L	6/8/9/11/47	7.29	-50	5	50	77
Medial Frontal Gyrus	L/R	6/8/9	7.25	-15	25	35	26
Insula	L	13	8.72	-35	5	20	51
Inferior Frontal Gyrus	L	9/44/45/47	8.23	-35	5	30	50
Cingulate Gyrus	L/R	24/32	8.61	-10	15	30	78
Anterior Cingulate	L/R	24/25/32/33	8.99	-5	20	20	44

Note. Region = region as labelled by sLORETA (50); Hemisphere = hemisphere of the cluster (L = left, R = right; note that bilateral clusters with voxels that were not separated by at least 10 mm were counted as one cluster); BA = Brodmann area of maximum t-value(s); tmax = maximum t-value within a cluster; x, y, z = MNI coordinates; Voxels = number of activated voxels within the cluster. Table showing regions with at least 10 significantly activated voxels (alpha level: 1%, one-tailed, NoGo > Go, whole-brain corrected).

Table S6

Grand-Mean Microstates Maps in Study 2

Microstate	A	B	C	D
Map				
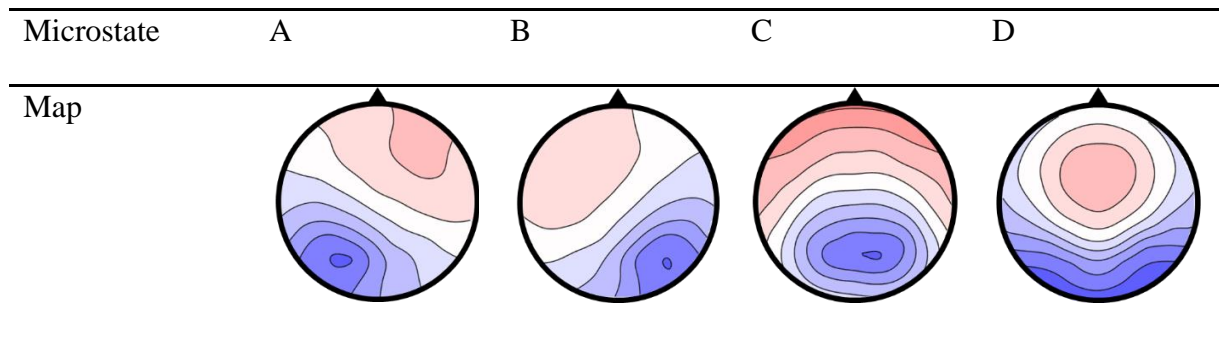
Note. Grand-mean maps of resting-state microstates in Study 2 (for descriptive statistics

see Table S7 in the supplementary material). Note the high similarity with the grand-

mean microstate maps obtained from our original German sample (Study 1; see Figure 1).

Table S7

Descriptive Statistics of all Variables in Study 2

Variable	Min	Max	Mean	SD
Measures of self-control				
Self-reported self-control (BSCS)	18	59	39.12	8.73
Risk-taking behavior (BART)	.13	12.68	3.91	2.73
Characteristics of resting-state microstates				
Duration network A	20.63	84.49	47.20	13.10
Duration network B	13.03	76.17	44.86	11.50
Duration network C	15.68	78.73	48.63	13.34
Duration network D	20.25	85.15	48.03	14.39
Mean duration A-D	20.25	80.47	47.69	11.99
Occurrence network A	3.14	15.47	5.63	1.93
Occurrence network B	2.37	11.59	5.29	1.75
Occurrence network C	2.92	15.25	5.86	1.84
Occurrence network D	3.25	15.26	5.76	2.01
Mean occurrence A-D	12.43	49.39	22.54	6.77

Note. $N = 101$. Min = minimum value, Max = maximum value, Mean = mean value, SD = standard deviation.

Table S8

Correlations of Study 2

	Self-reported self-control		Risk-taking behavior	
Microstate characteristics	*r*	*p*	*r*	*p*
Duration microstate A	**.282**	**.004**	**-.226**	**.023**
Duration microstate B	.125	.213	-.162	.106
Duration microstate C	.140	.164	**-.253**	**.011**
Duration microstate D	.169	.091	**-.273**	**.006**
Mean duration A-D	**.199**	**.046**	**-.253**	**.011**
Occurrence microstate A	-.060	.553	.167	.094
Occurrence microstate B	-.193	.053	**.312**	**.002**
Occurrence microstate C	-.149	.137	.173	.083
Occurrence microstate D	-.159	.113	.230	.021
Mean occurrence A-D	-.155	.123	**.244**	**.014**

Note. $N = 101$. r = Pearson correlation coefficient; p = p-value. Bold values indicate

significant correlations (two-sided, alpha level = .05). Note that 8/8 correlations of

microstate durations with self-reported self-control and risk-taking behavior are positive,

and 8/8 correlations of microstate occurrences with self-reported self-control and risk-

taking behavior are negative.

Table S9

Associations of the Mean Spectral Power of EEG Frequency Bands with Microstate

Duration and Indices of Self-Control

Predicting microstate duration with EEG frequency bands ($N = 159$)					
Predictors	b	SDE	$t(157)$	p	R^2_m
Mean delta power	.080	.066	1.21	.225	.007
Mean theta power	.227	.067	3.46	< .001	.052
Mean alpha power	.154	.055	2.79	.006	.025
Mean beta power	-.011	.064	-.166	.868	< .001

Predicting self-reported self-control with EEG frequency bands ($N = 159$)				
Predictors	β	$t(157)$	p	R^2
Mean delta power	.228	2.94	.004	.052
Mean theta power	.172	2.19	.030	.030
Mean alpha power	.104	1.31	.192	.011
Mean beta power	.042	.526	.599	.002

Predicting the neural index of inhibitory control with EEG frequency bands ($N = 58$)				
Predictors	β	$t(56)$	p	R^2
Mean delta power	.135	1.02	.313	.018
Mean theta power	.108	.816	.418	.012
Mean alpha power	.156	1.19	.241	.024
Mean beta power	.262	2.03	.047	.069

Predicting risk-taking behavior with EEG frequency bands ($N = 101$)

Predictors	β	$t(100)$	p	R^2
Mean delta power	.118	1.18	.239	.014
Mean theta power	-.037	-.373	.710	.001
Mean alpha power	-.090	-.900	.371	.008
Mean beta power	-.025	-.251	.802	< .001

Note. b = regression coefficient (linear mixed models), SDE = standard error (linear mixed models), β = standardized regression coefficient (linear regression analyses), t(df) = t-value (degrees of freedom), p = p-value, R^2_m = marginal R-squared value (linear mixed models), R^2 = R-squared value (linear regression analyses). Results of mixed model analyses testing for associations of the mean spectral power of EEG frequency bands in the resting-state EEG with microstate duration, and results of linear regression analyses testing for associations of the mean spectral power of EEG frequency bands with self-reported self-control ($N = 159$), the neural index of inhibitory control ($N = 58$) and risk-taking behavior ($N = 101$).

Table S10

Exemplary Linear Mixed Model Analysis in Study 1

Single predictor model (main effect)					
Predictor	*b*	*SDE*	*t(56)*	*p*	$R^2{}_m$
Self-control	.419	.095	4.41	< .001	**.177**

Interactions of microstate types with reference to type A					
Predictor	*b*	*SDE*	*t(56)*	*p*	$R^2{}_m$
Self-reported self-control	.237	.095	1.98	.053	
Interaction with dummy type B	.323	.117	2.77	.006	
Interaction with dummy type C	.223	.117	1.91	.058	
Interaction with dummy type D	.186	.117	1.59	.113	.190

Interactions of microstate types with reference to type B					
Predictor	*b*	*SDE*	*t(56)*	*p*	$R^2{}_m$
Self-reported self-control	.559	.095	4.68	< .001	
Interaction with dummy type A	-.323	.117	-2.77	.006	
Interaction with dummy type C	-.100	.117	-.856	.393	
Interaction with dummy type D	-.137	.117	-1.17	.242	.190

Interactions of microstate types with reference to type C					
Predictor	*b*	*SDE*	*t(56)*	*p*	$R^2{}_m$
Self-reported self-control	.460	.095	3.85	< .001	
Interaction with dummy type A	-.223	.117	-1.91	.058	
Interaction with dummy type B	.100	.117	.856	.393	.190

Interaction with dummy type D	-.037	.117	-.318	.751	

Interactions of microstate types with reference to type D

Predictor	*b*	*SDE*	*t(56)*	*p*	$R^2{}_m$
Self-reported Self-control	.422	.095	3.53	< .001	
Interaction with dummy type A	-.186	.117	-1.59	.113	
Interaction with dummy type B	.137	.117	1.17	.242	
Interaction with dummy type C	.037	.117	.318	.751	.190

Note. N = 58. b = regression coefficient, SDE = standard error, t(df) = t-value (degrees of freedom), p = p-value, $R^2{}_m$ = marginal R-squared value explained by the respective model. Exemplary linear mixed model analysis for the prediction of the duration of resting-state microstates across types with self-reported self-control using a dataset in long format with 4 observations per participant (due to 4 microstate types) and a random intercept across participants. First, only self-reported self-control is included in a single predictor model, illustrating a significant positive main effect. Next, interactions of self-reported self-control with dummy variables of microstate types are added to the model (e.g., the dummy variable of microstate A consists of ones for all characteristics of microstate A and zeros for all characteristics of microstate types other than A). These four additional interaction models allow for a direct comparison of associations between self-reported self-control and microstate durations with reference to one specific type (e.g., a positive coefficient of an interaction term indicates a stronger association of self-reported self-control with the duration of this specific network type compared to the reference type). Note, that main effects should be interpreted with caution in models including higher-level interaction-terms. In our example, adding interactions with

dummies leads to a significant increase in the model fit compared to the single-predictor model ($p = .046$), with additional variance being explained (increase of approximately 1.3%). Inspecting the data, we can draw the conclusion that the association of self-reported self-control with the duration of microstate B is significantly stronger compared to the association with the duration of microstate A (see interactions of network types with reference to type A; $b = .323$, $p = .006$). Note that this is equal to the conclusion that the association of self-reported self-control with the duration of microstate A is significantly weaker compared to the association with the duration of microstate B (interactions of network types with reference to type B; $b = -.323$, $p = .006$).

Table S11

Confirmation of Main Findings Controlling for Gender in Study 2

Predicting microstate duration with self-reported self-control and gender					
Predictors	*b*	*SDE*	*t(97)*	*p*	*R²ₘ*
Self-reported self-control	.204	.146	1.39	.167	
Gender	.241	.177	1.37	.175	
Self-reported self-control*gender	-.048	.181	-.264	.793	.047
Predicting microstate occurrence with self-reported self-control and gender					
Predictors	*b*	*SDE*	*t(97)*	*p*	*R²ₘ*
Self-control	-.156	.148	-1.05	.296	
Gender	-.171	.179	-.953	.343	
Self-reported self-control*gender	.032	.183	.173	.863	.026
Predicting microstate duration with risk-taking behavior and gender					
Predictors	*b*	*SDE*	*t(97)*	*p*	*R²ₘ*
Risk-taking behavior	-.215	.127	-1.69	.094	
Gender	.239	.174	1.37	.173	
Risk-taking behavior*gender	-.021	.172	-.124	.901	.067
Predicting microstate occurrence with risk-taking behavior and gender					
Predictors	*b*	*SDE*	*t(97)*	*p*	*R²ₘ*
Risk-taking behavior	.234	.128	1.83	.071	
Gender	-.167	.176	-.948	.345	
Risk-taking behavior*gender	-.031	.174	-.177	.860	.054

Note. $N = 101$. b = regression coefficient, SDE = standard error, t(df) = t-value (degrees of freedom), p = p-value, R^2_m = marginal R-squared value. Results of mixed model analyses testing for an interaction of the main effects of Study 2 with gender. There were no interactions of self-reported self-control or risk-taking behavior with gender in any of the models. As there were also no theoretical reasons to assume gender differences in fundamental resting-state microstates, we did not analyze these differences any further.

Table S12

Confirmation of Main Findings Controlling for Condition in Study 2

Predicting microstate duration with self-reported self-control and condition

Predictors	b	SDE	$t(97)$	p	R^2_m
Self-reported self-control	.230	.138	1.67	.098	
Condition	-.096	.178	-.540	.591	
Self-reported self-control* condition	-.091	.177	-.515	.608	.036

Predicting microstate occurrence with s self-reported elf-control and condition

Predictors	b	SDE	$t(97)$	p	R^2_m
Self-reported self-control	-.166	.139	-1.19	.236	
Condition	.008	.180	.044	.965	
Self-reported self-control*condition	.048	.179	.265	.791	.020

Predicting microstate duration with risk-taking behavior and condition

Predictors	b	SDE	$t(97)$	p	R^2_m
Risk-taking behavior	-.257	.121	-2.12	.037	
Condition	-.140	.176	-.798	.427	
Risk-taking behavior*condition	.046	.174	.267	.790	.058

Predicting microstate occurrence with risk-taking behavior and condition

Predictors	b	SDE	$t(97)$	p	R^2_m
Risk-taking behavior	.245	.122	2.00	.048	
Condition	.048	.177	.271	.787	
Risk-taking behavior*condition	-.049	.175	-.278	.782	.049

Note. $N = 101$. b = regression coefficient, SDE = standard error, t(df) = t-value (degrees of freedom), p = p-value, R^2_m = marginal R-squared value. Results of mixed model analyses testing for an interaction of the main effects of Study 2 with experimental conditions. There were no interactions of Self-reported self-control or risk-taking behavior with condition in any of the models, which is why we did not analyze these results any further.